Procedia Computer Science
Volume 66, 2015, Pages 200–209
YSC 2015. 4th International Young Scientists Conference on Computational Science

Mathematical modeling of a river stream based on a shallow water approach

Vladislava Churuksaeva[1], Alexander Starchenko[1]
[1]National Research Tomsk State University, Tomsk, Russia
chu.vv@mail.ru, starch@math.tsu.ru

Abstract

Flood control problems as well as problems connected with wastewater discharge into rivers are issues of current importance. Depth averaged shallow water equations are used to model flows where water depth is much less than the horizontal dimension of the computational area and the free surface greatly influences the flow.

The present work is focused on developing the mathematical model, applying the unsteady 2D shallow water equations, and constructing a numerical method for computing the river flow in extensive spatial areas.

A finite volume solver for turbulent shallow water equations is presented. Some computational examples were carried out to investigate the applicability of the model. The comparison between the numerical solution and experimental results shows that the depth averaged model correctly represents flow patterns in the cases described and nonlinear effects in a river flow.

Keywords: depth-averaged shallow water model, finite volume method, numerical modeling, river flow

1 Introduction

Numerical modeling of a river stream originated in the early 1920s and was connected with rapid development of fluid mechanics and the necessity to investigate the behavior of hydrological objects to construct hydraulic facilities.

Flow turbulence influence heat-mass exchange and should be taken into account to describe influence of horizontal mixing and near-bottom flows.

The first investigations of turbulence in river streams were performed to evaluate the accuracy of measurements of the mean flow velocity with devices. One of the first theoretical results of Soviet hydraulic engineers' work on turbulence was the "diffusive theory of turbulence" that was developed

 Selection and peer-review under responsibility of the Scientific Programme Committee of YSC 2015

doi:10.1016/j.procs.2015.11.024

in the 1930s to the 1960s. The basis of this theory consists of postulates introduced by Boussinesq in 1877 and Taylor and Schmitt in 1915-1925 (Sedov, 2013).

Since that time, increase in computational power has allowed creating mathematical models and methods that are more complex and more accurate, including methods for unsteady flows and flows in deformable beds (McGuirk & Rodi, 1978; Chu & Babarutsi , 1988; Yu & Zhu, 1993; Olsen & Stokseth, 1995; Hou, Simons, Mahgoub, & Hinkelmann, 2013).

As the computational cost of numerical modeling of the flow in a river or an estuary even with 2D depth-averaged equations with simple turbulence models is very high, elementary one-dimensional computational models are still widely used for computations in large domains or to get approximate data about transport of pollutants (Finaud-Guyot, Delenne, Guinot, & Llovel, 2011; Lyubimova, Lepihin, & Parshakova, 2010). Additionally, computational results obtained from the one-dimensional model can be used as boundary conditions for computations with a 2D or 3D model. But in conditions of ice movement or flood propagation problems, where the flow is usually unsteady and wet-dry fronts are present, the accuracy of these methods is not high enough.

The most general approach to model free surface flows is to solve the fully 3D flow field with specific treatment of the free surface and bottom boundary conditions, but review of the literature shows that 3D models are either used with the LES method (Chaouat & Schiestel, 2002; Kang, Lightbody, Hill, & Sotiropoulos, 2011), or used for small-scale flow computations in a laboratory (Kang, Lightbody, Hill, & Sotiropoulos, 2011; Kang & Sotiropoulos, 2012) or a short river section adjacent to hydraulic facilities where highly accurate prediction of hydrodynamic processes is essential (Sandiv, Sotiropoulos, & Odgaard, 1998; Olsen & Stokseth, 1995). In Sandiv, Sotiropoulos, & Odgaard (1998) 3D SWE are applied to modeling a river stream in a $4km$-long stretch of the Columbia River adjacent to a dam. These authors state that it is the first work in which a 3D model is applied to modeling a river flow without any simplifications, except in Olsen & Stokset (1995), where flow in a small (20 m to 40 m) river section was modeled.

But in river engineering applications, solving 3D equations is not reasonable due to significant difference in the scales of the processes, the extensiveness of spatial domain, and the complex geometry of the border.

An alternative approach involves simplifying 3D Reynolds averaged Navier-Stokes equations in order to obtain the depth-averaged shallow water equations.

There are many works on turbulent flow computations using depth averaged shallow water equations that deal with flows in rivers and estuaries and use models with Coriolis force and wind force and take into account the extensiveness of the area studied (Yu & Zhu, 1993; Sauvaget, David, & Soares, 2000; River2D Hydrodynamic Model for Fish Habitat, 2002; Hou, Simons, Mahgoub, & Hinkelmann, 2013). This problem is discussed in detail in Duc, Wenka, & Rodi (2004) and Uijttewaal (2014).

The present work is focused on developing the mathematical model and a numerical method for computing the river flow in extensive spatial areas. The model constructed should give accurate values of turbulent flow parameters to get an accurate prediction of transport of pollutants and flood propagation.

2 Governing equations

The mathematical model is based on depth averaged Reynolds equations for viscous flow. It is assumed that the distribution of pressure is hydrostatic and flow characteristics vary little with depth, and that the water depth is much less than the horizontal dimensions of the field of research, thus limiting the formation of three-dimensional vortexes and defining the two-dimensional nature of turbulence.

$$\frac{\partial h}{\partial t}+\frac{\partial (h\bar{u})}{\partial x}+\frac{\partial (h\bar{v})}{\partial y}=0,$$

$$\frac{\partial (h\bar{u})}{\partial t}+\frac{\partial (h\bar{u}^2)}{\partial x}+\frac{\partial (h\bar{u}\,\bar{v})}{\partial y}=-gh\frac{\partial (z_b+h)}{\partial x}+\frac{1}{\rho}\frac{\partial (h\bar{\tau}_{xx})}{\partial x}+\frac{1}{\rho}\frac{\partial (h\bar{\tau}_{xy})}{\partial y}+\frac{(\tau_{xz})_s-(\tau_{xz})_b}{\rho}-\bar{F}_x,$$

$$\frac{\partial (h\bar{v})}{\partial t}+\frac{\partial (h\bar{u}\,\bar{v})}{\partial x}+\frac{\partial (h\bar{v}^2)}{\partial y}=-gh\frac{\partial (z_b+h)}{\partial y}+\frac{1}{\rho}\frac{\partial (h\bar{\tau}_{yx})}{\partial x}+\frac{1}{\rho}\frac{\partial (h\bar{\tau}_{yy})}{\partial y}+\frac{(\tau_{yz})_s-(\tau_{yz})_b}{\rho}-\bar{F}_y,$$

where $h(x,y,t)$ is the water depth, $\bar{u}(x,y,t)$, $\bar{v}(x,y,t)$ are the depth averaged horizontal velocities; $z_b(x,y)$ is the bed elevation; ρ is the density, $g=9.81m/s^2$ is the gravity acceleration; $\bar{\tau}_{xx},\bar{\tau}_{xy},\bar{\tau}_{yx},\bar{\tau}_{yy}$ are the depth averaged components of the viscous stresses and Reynolds stresses tensor; $(\tau_{xz})_s,(\tau_{yz})_s,(\tau_{xz})_b,(\tau_{yz})_b$ are the wind stress and bottom friction, correspondingly; $\bar{F}_x,\bar{F}_y$ are the depth averaged Coriolis force components.

There are many methods for obtaining the stresses tensor's components $\bar{\tau}_{ij}$ from results of measurements. Semi-empirical models with algebraic (as in the Boussinesq Hypothesis) or geometric (as in the Prandtl Hypothesis) considerations about the value of turbulent viscosity are widely utilized in engineering calculations (River2D Hydrodynamic Model for Fish Habitat, 2002; Yu & Zhu, 1993). A significant disadvantage of these models is the assumption on the local turbulence equilibrium, which is inadequate to present the effects of the transfer and flow history. To account for production, transport, and dissipation of turbulence, differential turbulence models were developed. In this approach transport equations are included to the flow model to describe the transfer of turbulence parameters. Turbulence models for the depth-averaged shallow water model are not as developed as models for classic Reynolds equations but there are several widely used and well-tested models such as the depth averaged $k-\varepsilon$ model (Rodi, 1984; Cea & Vazquez-Cendon, 2012), depth averaged $k-\omega$ model (Yu & Righetto, 2001), and models with a constant diffusion coefficient or simple algebraic relations to obtain it (River2D Hydrodynamic Model for Fish Habitat, 2002; Cea, Puertas, & Vazquez-Cendon, 2007). Depth averaged stresses $\bar{\tau}_{ij}$ are obtained from the Boussinesq Assumption

$$\frac{1}{\rho}\bar{\tau}_{ij}=\left(\nu+\bar{\nu}_t\right)\left(\frac{\partial \bar{u}_i}{\partial x_j}+\frac{\partial \bar{u}_j}{\partial x_i}\right)-\frac{2}{3}\bar{k}\,\delta_{ij},$$

Eddy viscosity $\bar{\nu}_t$ and turbulence kinetic energy $\bar{k}$ are obtained from depth averaged high Reynolds ($\bar{\nu}_t \gg \nu$) $k-\varepsilon$ model (Rodi, 1984)

$$\bar{\nu}_t=c_\mu\frac{\bar{k}^2}{\bar{\varepsilon}},$$

$$\frac{\partial\left(h\tilde{k}\right)}{\partial t}+\frac{\partial\left(h\bar{u}\tilde{k}\right)}{\partial x}+\frac{\partial\left(h\bar{v}\tilde{k}\right)}{\partial y}=\frac{\partial}{\partial x}\left(h\frac{\bar{\nu}_t}{\sigma_k}\frac{\partial \tilde{k}}{\partial x}\right)+\frac{\partial}{\partial y}\left(h\frac{\bar{\nu}_t}{\sigma_k}\frac{\partial \tilde{k}}{\partial y}\right)+\left(P_h+P_{kv}-\tilde{\varepsilon}\right)h,$$

$$\frac{\partial\left(h\tilde{\varepsilon}\right)}{\partial t}+\frac{\partial\left(h\bar{u}\tilde{\varepsilon}\right)}{\partial x}+\frac{\partial\left(h\bar{v}\tilde{\varepsilon}\right)}{\partial y}=\frac{\partial}{\partial x}\left(h\frac{\bar{\nu}_t}{\sigma_\varepsilon}\frac{\partial \tilde{\varepsilon}}{\partial x}\right)+\frac{\partial}{\partial y}\left(h\frac{\bar{\nu}_t}{\sigma_\varepsilon}\frac{\partial \tilde{\varepsilon}}{\partial y}\right)+\left(c_1\frac{\tilde{\varepsilon}}{\tilde{k}}P_h+P_{\varepsilon v}-c_2\frac{\tilde{\varepsilon}^2}{\tilde{k}}\right)h,$$

where $P_h=\bar{\nu}_t\left[2\left(\frac{\partial \bar{u}}{\partial x}\right)^2+2\left(\frac{\partial \bar{v}}{\partial y}\right)^2+\left(\frac{\partial \bar{u}}{\partial y}+\frac{\partial \bar{v}}{\partial x}\right)^2\right]$,

$\sigma_\varepsilon=1.3;\sigma_k=1.0;c_1=1.44;c_2=1.92;c_\mu=0.09;$

$$P_{kv} = c_k \frac{v_*^3}{h}; P_{\varepsilon v} = c_\varepsilon \frac{v_*^4}{h^2}; c_k = \frac{1}{\sqrt{c_f}}; c_\varepsilon = 3.6 \frac{c_2}{c_f^{3/4}} \sqrt{c_\mu}; c_f = \frac{gn^2}{h^{1/3}}.$$

Here n is the Manning coefficient.

As $\bar{v}_t \gg v$ does not hold near the wall, where it adsorbs the fluctuations, Launder-Spalding wall functions are used to define stresses.

The advection-diffusion equation

$$\frac{\partial(h\bar{c})}{\partial t} + \frac{\partial(h\bar{u}\,\bar{c})}{\partial x} + \frac{\partial(h\bar{v}\,\bar{c})}{\partial y} = \frac{\partial}{\partial x}\left(h\bar{\Gamma}_t \frac{\partial \bar{c}}{\partial x}\right) + \frac{\partial}{\partial y}\left(h\bar{\Gamma}_t \frac{\partial \bar{c}}{\partial y}\right)$$

where $h(x, y, t)$ is the water depth, $\bar{c}(x, y, t)$ is the depth-averaged concentration of pollutants, and $\bar{\Gamma}_t(x, y, t)$ is the turbulence diffusivity, is added into the set of equations to mathematically simulate a possible scenario of the transport of pollutants from environmental sources and enterprises into the surface water of rivers, which is essential for predicting and monitoring of the river ecosystem.

Due to the fact that in this situation the discharged mass is relatively small (in comparison to the mass of the flowing water) and is flowing in the river at a low speed, the three-dimensional turbulent effects do not occur near the site of its ejection.

Variables distribution is assumed to be homogeneous at the inflow boundary of the flow domain. Simple gradient boundary conditions are used at the outlet boundary. No-slip boundary conditions and Launder and Spalding wall functions for turbulence characteristics and friction are used at the solid boundaries.

3 A finite volume solver

In this section a finite volume method on a staggered rectangular grid is used to discretize the difference equations. The water depth is defined at the cell centers, velocity components are defined at the midpoints of control volume edges.

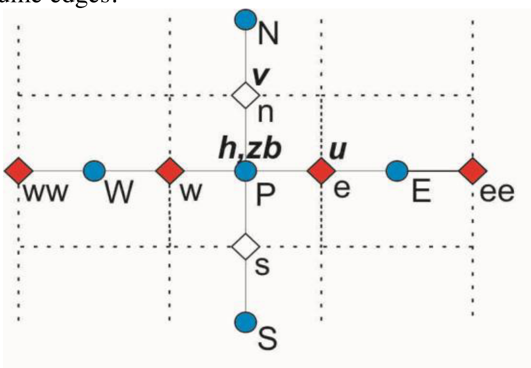

Figure 1 Control volume and mesh stencil

MLU and MUSCL schemes (Van Leer, 1979) are used to approximate the convective terms. As processes are developing slowly we consider an implicit method to be preferable.

An iterative algorithm for solving depth-averaged shallow water equations with unknowns $h(x,y,t), \bar{u}(x,y,t), \bar{v}(x,y,t)$ has been constructed based on the procedure proposed by Patankar and Spalding for the Reynolds equations (Patankar, 1980). First we obtain the formulas of the algorithm.

Initial values of $h(x,y,t), \bar{u}(x,y,t), \bar{v}(x,y,t)$ at every time step are supposed to be equal to correspondent values from the previous time step. Refinement of the solution, which satisfies the shallow water equations at each time step, will be carried out by an iterative procedure. This procedure allows avoiding spurious oscillations and obtaining the correct numerical solution for the fields of velocity and depth.

The velocity components are calculated from the following difference equations using the initial values of flow depth.

$$a_e^u \bar{u}_e^* = \sum_{nb} a_{nb}^u \bar{u}_{nb}^* + d_e^u \left(h_E^i - h_P^i \right) + b_e^u; \tag{1}$$

$$a_n^v \bar{v}_n^* = \sum_{nb} a_{nb}^v \bar{v}_{nb}^* + d_n^v \left(h_N^i - h_P^i \right) + b_n^v. \tag{2}$$

Here $\bar{u}_e^*$, $\bar{v}_n^*$ are the interim values of the velocity components that do not satisfy, in general, the continuum difference equation. (Patankar, 1980)

It is required that at the next iteration all the equations are satisfied, that is

$$a_e^u \bar{u}_e^{i+1} = \sum_{nb} a_{nb}^u \bar{u}_{nb}^{i+1} + d_e^u \left(h_E^{i+1} - h_P^{i+1} \right) + b_e^u;$$

$$a_n^v \bar{v}_n^{i+1} = \sum_{nb} a_{nb}^v \bar{v}_{nb}^{i+1} + d_n^v \left(h_N^{i+1} - h_P^{i+1} \right) + b_n^v.$$

Subtracting these equations from corresponding previous ones, and omitting the terms $\sum_{nb} a_{nb}^u \left(\bar{u}_{nb}^{i+1} - \bar{u}_{nb}^* \right)$, $\sum_{nb} a_{nb}^v \left(\bar{v}_{nb}^{i+1} - \bar{v}_{nb}^* \right)$, as in Patankar (1980), we get

$$\bar{u}_e^{i+1} = \bar{u}_e^* + d_e^u / a_e^u \left(h_E' - h_P' \right); \tag{3}$$

$$\bar{v}_n^{i+1} = \bar{v}_n^* + d_n^v / a_n^v \left(h_N' - h_P' \right), \tag{4}$$

where $h_P' = h_P^{i+1} - h_P^i$.

The equation for $\left\{ h_P' \right\}$ is obtained from the difference continuity equation

$$\frac{h_P^{i+1} - h_P^0}{\tau} + \frac{\bar{u}_e^{i+1} h_e^i - \bar{u}_w^{i+1} h_w^i}{\delta x} + \frac{\bar{v}_n^{i+1} h_n^i - \bar{v}_s^{i+1} h_s^i}{\delta y} = 0,$$

and will be

$$\begin{gathered} \frac{h_P' + h_P^i - h_P^0}{\tau} + \frac{h_e^i}{\delta x}\left(\bar{u}_e^* + \frac{d_e^u}{a_e^u}\left(h_E' - h_P' \right) \right) - \frac{h_w^i}{\delta x}\left(\bar{u}_w^* + \frac{d_w^u}{a_w^u}\left(h_P' - h_W' \right) \right) \\ \frac{h_n^i}{\delta y}\left(\bar{v}_n^* + \frac{d_n^v}{a_n^v}\left(h_N' - h_P' \right) \right) + \frac{h_s^i}{\delta y}\left(\bar{v}_s^* + \frac{d_n^v}{a_n^v}\left(h_P' - h_S' \right) \right) = 0. \end{gathered} \tag{5}$$

Thus, at each time step following steps are repeated:

1. Setting $\bar{u}^i = \bar{u}^0$, $\bar{v}^i = \bar{v}^0$, $h^i = h^0$.
2. Solving (1), (2) with the successive over-relaxation method to obtain $\left\{ \bar{u}^* \right\}$, $\left\{ \bar{v}^* \right\}$.
3. Solving (5) with the successive over-relaxation method to obtain $\left\{ h_P' \right\}$.
4. Correcting $\left\{ \bar{u}^{i+1} \right\}$, $\left\{ \bar{v}^{i+1} \right\}$ with (3), (4) and $\left\{ h^{i+1} \right\}$ with $h_P^{i+1} = h_P^i + h_P'$.
5. If $\left\| \bar{h}' \right\|$ is great, then $i = i + 1$ and return to step 2 (repeat iterations until $\left\| h' \right\| > \varepsilon$).

The proposed method is different from the widely used SIMPLE-based method, as depth variability is taken into account in the continuity equation.

4 Results and discussion

Some test cases that illustrate the different flow patterns were carried out using this method to investigate the influence of bottom friction and bottom elevation. As a validation of a mathematical model and numerical method, the results have been compared with experimental data and calculations given in Cea, Puertas, & Vazquez-Cendon (2007) and McGuirk & Rodi (1978). A comparison helps to define whether the shallow water hypothesis is applicable to the modeling of turbulent river flow.

One common application of the 2D shallow water model is modeling open channel flows. Abrupt change of flow direction can produce 3D turbulence effects that can deteriorate numerical predictions given by the depth-averaged equations.

In this section free surface flow in an open channel with a 90° bend is computed. The first section is $0.86m$ wide with a flat bottom, and the second section is $0.72m$ wide with flat bottom. At the end of the first section there is a step with a change in the bed elevation of $0.013m$. The mean water depth is $h \approx 0.175m$. The horizontal velocities are of the order of $0.2m/s$.

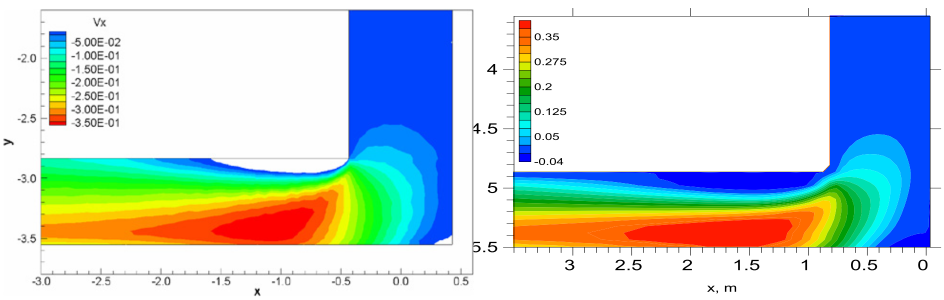

a b

Figure 2 The fields of velocity x-component obtained in Cea, Puertas, & Vazquez-Cendon (2007) with the Roe Scheme and $k-\varepsilon$ turbulence model (a) and in this work with the method presented (b)

Comparison shows that the mathematical model correctly detects the large recirculation region downstream from the bend and a small recirculation region in an external corner of the channel.

A comparison of the numerical and experimental fields is done in a cross-section downstream from the bend at $y = 1.23m$ for a more detailed investigation of the numerical results and to test the influence of the approximation of convective terms in a motion equation. Figure 3 shows the longitudinal velocity and kinetic energy of turbulence in the cross-section of the channel, where a there is the region of recirculating flow.

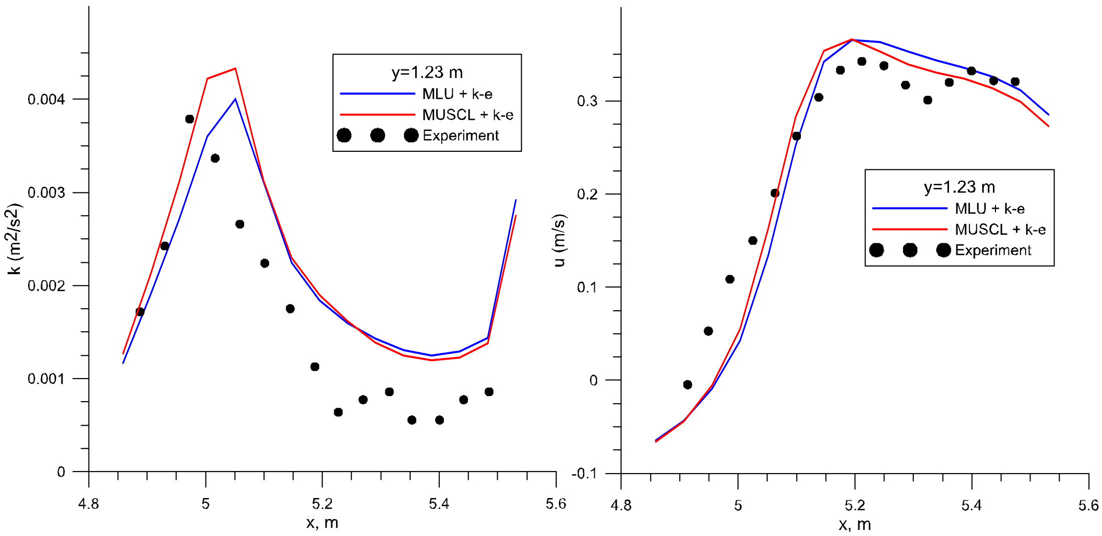

Figure 3 Comparison of the measured values presented in Cea, Puertas & Vazquez-Cendon (2007) (marks) with the authors' predicted values (lines) of kinetic turbulence energy and longitudinal velocity downstream from the bend

Figure 3 shows that the mathematical model and numerical method presented above correctly predict the distribution of a longitudinal velocity and turbulence kinetic energy across the channel. The higher-order scheme for the convective terms provides a solution that is closer to the experimental data.

The method proposed has been also applied to modeling steady turbulent flow in a small shallow river with sharply curved banks (Figure 4).

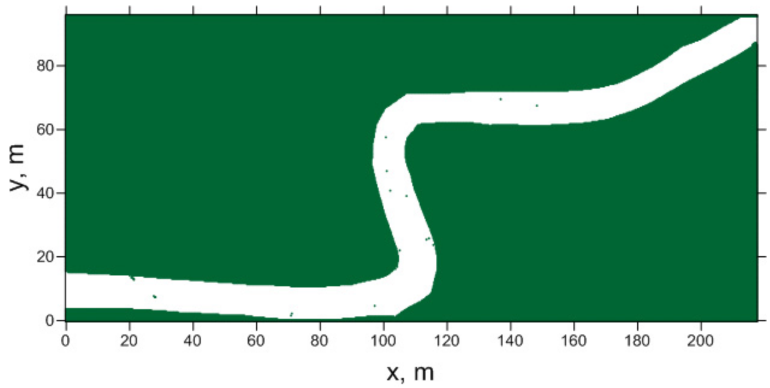

Figure 4 Geometry of the river studied

The bed is approximately $12m$ wide. The flow velocity is set to $0.7m/s$ at the inlet boundary, and the water depth is set to $0.3m$ at the outlet boundary. The river has a complex bathymetry and small irregularities with horizontal dimensions of the order of $0.3-0.5m$ that are above the water and randomly placed in the bed. The Manning coefficient is set to 0.02. A structured uniform mesh with 802×282 nodes is used for computations. The convergence of the iterative process is controlled with the value of water discharge at the outlet of the domain.

Figure 5 shows the distribution of the depth-averaged velocity magnitude at the central part of the domain with the abrupt change in flow direction.

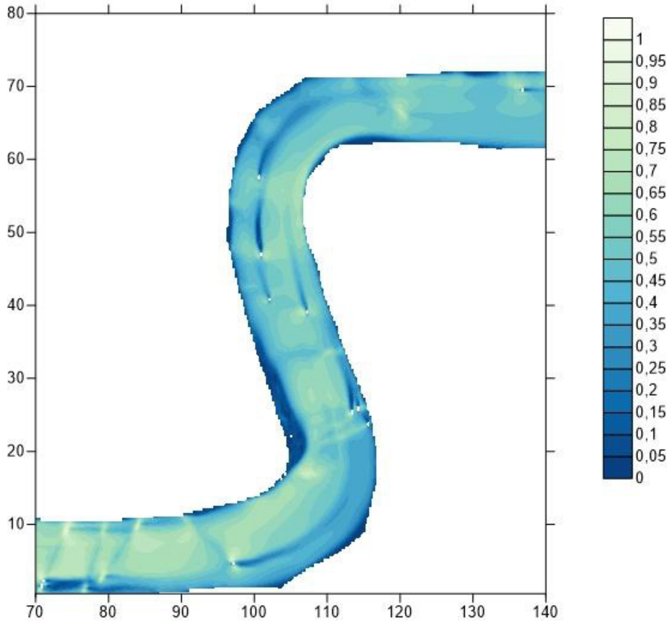

Figure 5 Depth-averaged velocity magnitude distribution. To the right is the scale of values in m/s.

This figure shows that the turbulent flow in the curved riverbed has common characteristics with the open channel flow in a bend (Figure 2). There is the large recirculation region after the first bend, and the flow tends to move to the opposite bank. But existing irregularities of the river's bottom destroy this structure of the flow, causing the stream to move along the path of least resistance, avoiding elevations. It especially shows up before the second bend, where a ridge of irregularities is. Figure 5 also shows that the flow accelerates over the bottom rises and slows down over small hollows.

5 Conclusions

In this paper we have presented the mathematical model and the numerical method for studying turbulent river flow based on the shallow water approach. The model takes into account bed and wind friction, Coriolis force, and river geometry with side inflows and complex bathymetry. The depth-averaged modification of the two-parameter $k-\varepsilon$ turbulence model with additional terms to take into account the turbulence production due to the bottom friction has been added to the mathematical model to describe the turbulent structure of the flow. The numerical method proposed is the modification of the Patankar's SIMPLE algorithm with additional accounting for the depth variation in convective and diffusive terms of the momentum equations.

The mathematical model and the solver proposed have been applied to modeling the free surface flow in an open channel with a 90° bend and the flow in a shallow river with randomly located obstacles. The results of computations in the laboratory channel show a good agreement with the experimental observations and results from the works cited by us on the values of both velocity and turbulence energy. The analysis of the results shows that higher quality of prediction of the values observed in the recirculation flows can be achieved by applying a higher-order numerical scheme for convective terms in transport equations.

The results of the calculations of the flow in the S-shaped river with obstacles represent flow patterns observed in studying river flows and show agreement with general concepts.

6 Acknowledgement

This work was financially supported by the Ministry of Education and Science of the Russian Federation, project № 5.628.2014 / K.

The authors wish to thank Jean Kollantai (Senior Lecturer at Tomsk State University) for her assistance with the style of the paper.

References

Cea, L., & Vazquez-Cendon, M. (2012). Unstructured finite volume discretisation of bed friction and convective flux in solute transport models linked to the shallow water equations. *Journal of Computational Physics* (231), pp. 3317-3339.

Cea, L., Puertas, J., & Vazquez-Cendon, M.-E. (2007, September). Depth averaged modelling of turbulent shallow water flow with wet-dry fonts. *Archives of Computational Methods in Engineering , 14* (3), pp. 303-341.

Chaouat, B., & Schiestel, R. (2002). Reynolds stress transport modelling for steady and unsteady channel flows with wall injection. *Journal of Turbulence , 3*, pp. 1-16.

Chu, V. H., & Babarutsi , S. (1988). Confinement and bed-friction effects in shallow turbulent mixing layers. *Journal of Hydraulic Engineering , 10* (114), pp. 1257-1274.

Duc, B., Wenka, T., & Rodi, W. (2004, September). Numerical modeling of bed deformation in laboratory channels. *Journal of Hydraulic Engineering , 9*, pp. 894-904.

Finaud-Guyot, P., Delenne, C., Guinot, V., & Llovel, C. (2011). 1D–2D coupling for river flow modeling. *Comptes Rendus Mecanique* (339), pp. 226-234.

Hou, J., Simons, F., Mahgoub, M., & Hinkelmann, R. (2013). A robust well-balanced model on unstructured grids for shallow water flows with wetting and drying over complex topography. *Computer Methods in Applied Mechanics and Engineering* (257), pp. 126-149.

Kang, S., & Sotiropoulos, F. (2012). Numerical modeling of 3D turbulent free surface flow in natural waterways. *Advances in Water Resources* (40), pp. 23-36.

Kang, S., Lightbody, A., Hill, C., & Sotiropoulos, F. (2011). High-resolution numerical simulation of turbulence in natural waterways. *Advances in Water Resources , 34*, pp. 98-113.

Lyubimova, T. P., Lepihin, A. P., & Parshakova, Y. A. (2010). Tiunov, A. I. (2010). Chislennoe modelirovanie razbavleniya i perenosa vysokomineralizovannyh rassolov v turbulentnyh potokah. *Vychislitel'naya mekhanika sploshnyh sred* , pp. 68-79.

McGuirk, J. J., & Rodi, W. (1978). A depth-averaged mathematical model for the near field of side discharges into open channel flow. *Journal of Fluid Mechanics , 88*, pp. 761-781.

Olsen, N. R., & Stokseth, S. (1995). Three-dimensional numerical modelling of water flow in a river with large bed roughness. *Journal of Hydraulic Research , 33*, pp. 571-581.

Patankar, S. V. (1980). Numerical heat transfer and fluid flow. Hemisphere Publishing Corporation. *River2D Hydrodynamic Model for Fish Habitat*. (2002). Retrieved 2015 10-06 from River2D: http://www.river2d.ualberta.ca/

Rodi, V. (1984). Models of turbulence in the environment (Modeli turbulentnosti okruzhayuscheiy srediy). *Methods of Measuring Turbulent Flows (Metodi rascheta turbulentikh techenii)* , pp. 276-378.

Sandiv, S. K., Sotiropoulos, F., & Odgaard, A. J. (1998 January). Three-dimensional numerical model for flow through natural rivers. *Journal of Hydraulic Engineering , 124* (1), pp. 13-24.

Sauvaget, P., David, E., & Soares, C. (2000). Modelling tidal currents on the coast of Portugal. *Coastal Engineering* (40), pp. 393-409.

Sedov, L. I. (2013). *Mekhanika v SSSR za 50 let*. Moskva: Ripol Klassik.

Uijttewaal , W. (2014). Hydrodynamics of shallow flows: application to rivers. *Journal of Hydraulic Research , 52* (2), pp. 157-172.

Uijttewaal, W., & Booij, R. (2000). Effects of shallowness on the development. *Physics of Fluids , 2* (12), pp. 392-402.

Van Leer, B. (1979). Towards the ultimate conservative difference scheme. *Journal of Computational Physics* , pp. 10-136.

Yu, L., & Righetto, A. M. (2001). Depth-averaged k-omega turbulence model and application. *Advances in Engineering Software* (32), pp. 375-394.

Yu, L., & Zhu, S. P. (1993). Numerical simulation of discharged waste heat and contaminants into the south estuary of the Yangtze River. *Mathematical and Computer Modelling , 18* (12), pp. 107-123.